

## RESEARCH ARTICLE

# A mechanistic model of methane emission from animal slurry with a focus on microbial groups

Frederik R. Dalby<sup>1\*</sup>, Sasha D. Hafner<sup>1,2\*</sup>, Søren O. Petersen<sup>3</sup>, Andrew Vanderzaag<sup>4</sup>, Jemaneh Habtewold<sup>4</sup>, Kari Dunfield<sup>5</sup>, Martin H. Chantigny<sup>6</sup>, Sven G. Sommer<sup>1\*</sup>

**1** Department of Biotechnology and Chemical Engineering, Faculty of Technical Sciences, Aarhus University, Aarhus, Denmark, **2** Hafner Consulting LLC, Reston, Virginia, United States of America, **3** Department of Agroecology, Aarhus University, Tjele, Denmark, **4** Ottawa Research and Development Centre, Agriculture and Agri-Food Canada, Ottawa, Canada, **5** School of Environmental Science, University of Guelph, Guelph, Canada, **6** Quebec Research and Development Centre, Agriculture and Agri-Food Canada, Quebec, Canada

\* [sasha@hafnerconsulting.com](mailto:sasha@hafnerconsulting.com) (SDH); [fd@bce.au.dk](mailto:fd@bce.au.dk) (FRD); [sgs@bce.au.dk](mailto:sgs@bce.au.dk) (SGS)



## OPEN ACCESS

**Citation:** Dalby FR, Hafner SD, Petersen SO, Vanderzaag A, Habtewold J, Dunfield K, et al. (2021) A mechanistic model of methane emission from animal slurry with a focus on microbial groups. *PLoS ONE* 16(6): e0252881. <https://doi.org/10.1371/journal.pone.0252881>

**Editor:** Huan Li, Tsinghua University, CHINA

**Received:** November 17, 2020

**Accepted:** May 25, 2021

**Published:** June 10, 2021

**Copyright:** © 2021 Dalby et al. This is an open access article distributed under the terms of the [Creative Commons Attribution License](https://creativecommons.org/licenses/by/4.0/), which permits unrestricted use, distribution, and reproduction in any medium, provided the original author and source are credited.

**Data Availability Statement:** The data underlying the results presented in the study are available from GitHub at <https://github.com/sashahafner/ABM-paper>.

**Funding:** This work was funded by the Danish Agricultural Agency under the Ministry of Environment and Food (Miljø- og Fødevareministeriet) (grant no. 33010-NIFA-19-725). The funder provided support in the form of salaries for authors FRD, SDH, and SGS, but did not have any additional role in the study design, data collection and analysis, decision to publish, or

## Abstract

Liquid manure (slurry) from livestock releases methane (CH<sub>4</sub>) that contributes significantly to global warming. Existing models for slurry CH<sub>4</sub> production—used for mitigation and inventories—include effects of organic matter loading, temperature, and retention time but cannot predict important effects of management, or adequately capture essential temperature-driven dynamics. Here we present a new model that includes multiple methanogenic groups whose relative abundance shifts in response to changes in temperature or other environmental conditions. By default, the temperature responses of five groups correspond to those of four methanogenic species and one uncultured methanogen, although any number of groups could be defined. We argue that this simple mechanistic approach is able to describe both short- and long-term responses to temperature where other existing approaches fall short. The model is available in the open-source R package ABM (<https://github.com/sashahafner/ABM>) as a single flexible function that can include effects of slurry management (e.g., removal frequency and treatment methods) and changes in environmental conditions over time. Model simulations suggest that the reduction of CH<sub>4</sub> emission by frequent emptying of slurry pits is due to washout of active methanogens. Application of the model to represent a full-scale slurry storage tank showed it can reproduce important trends, including a delayed response to temperature changes. However, the magnitude of predicted emission is uncertain, primarily as a result of sensitivity to the hydrolysis rate constant, due to a wide range in reported values. Results indicated that with additional work—particularly on the magnitude of hydrolysis rate—the model could be a tool for estimation of CH<sub>4</sub> emissions for inventories.

preparation of the manuscript. The specific roles of these authors are articulated in the 'author contributions' section. Author SDH is employed by a commercial company: Hafner Consulting LLC.

**Competing interests:** The authors declare no competing interests. The affiliation of author SDH with a commercial company does not alter our adherence to PLOS ONE policies on sharing data and materials.

## Introduction

Methane ( $\text{CH}_4$ ) emissions from livestock production make a significant contribution to global warming, and manure management on farms contributes about 6.5% of global anthropogenic  $\text{CH}_4$  emissions [1, 2]. Current emissions estimates in national inventories are based on guidelines from the IPCC [3], which offer a simple "Tier 1" approach with default emission factors for livestock categories and average annual temperature, and a more detailed "Tier 2" approach considering effects of organic matter (as volatile solids, VS) loading, retention time, and temperature, i.e., properties that vary with farming practices and location. Tier 2 estimates are currently based on a modification of the model presented by Mangino et al. [4], in which the fraction of VS converted to  $\text{CH}_4$  within each month is calculated from a van 't Hoff-Arrhenius equation with an empirical estimate of activation energy and a reference point corresponding to 100% degradable VS conversion at 30 or 35°C. Although this provides a more site-specific estimate of  $\text{CH}_4$  emissions than fixed emission factors, the method has been found to poorly describe both temporal dynamics and total  $\text{CH}_4$  emissions in farm- and pilot-scale experiments [5–7]. Thus, a more accurate approach is needed to describe and quantify  $\text{CH}_4$  production in manure environments.

Models with a dynamic description of microbial decomposition of organic matter in anaerobic digesters already exist [8–11]. The ADM1 model was originally developed for anaerobic digestion almost two decades ago [10], and it remains a useful and popular tool for research and possibly even plant management [12, 13]. Despite its complexity (at least 26 differential equations), ADM1 and similar models were not developed to predict responses to temperature change known to affect  $\text{CH}_4$  production in stored slurry. The distinction between short- and long-term responses to environmental changes is also not included in these or most other models, which therefore cannot be used to assess slurry management practices such as cooling as a means to reduce  $\text{CH}_4$  emissions, or even for accurate estimation of seasonal variations. For example, an empirical model that accounted for daily temperature and VS degradation still failed to capture the observed dynamics of  $\text{CH}_4$  emissions, and it was concluded that the description of methanogenic activity under variable slurry storage conditions was inadequate [5].

In storage experiments with both fresh and aged slurry, a period of days to months with low  $\text{CH}_4$  emission rates has often been observed [5, 14–18]. Such a lag phase may reflect the time required for substrates of methanogenesis to reach a threshold concentration supporting growth, or the time required for development of an adapted methanogenic community. Some studies have highlighted the importance of residual aged manure in a storage acting as an inoculum, which suggests that community development is central for the temporal dynamics of  $\text{CH}_4$  emissions [19–21]. Thus, short-term changes due to temperature variation may reflect the activity of an existing methanogenic community, while long-term changes include the effects of successional changes of the community. Recent measurements of  $\text{CH}_4$  production rates in manure and digestate at temperatures between 5 and 52°C [22] highlight the difference between short- and long-term responses. These measurements show that the short-term (hours to days) response to a change in temperature is generally a shift away from the optimum of the active methanogenic community, but over time the activity at the new temperature will increase (Fig 1). Although some of the long-term differences in  $\text{CH}_4$  production were undoubtedly due to changes in substrate availability, considering them would tend to magnify the differences between short- and long-term responses. The general trend shown in Fig 1 is typical in studies of temperature change during anaerobic digestion [23–26].

The distinction between short- and long-term temperature responses was recently quantitatively addressed through development of an anaerobic digester model that included gradual

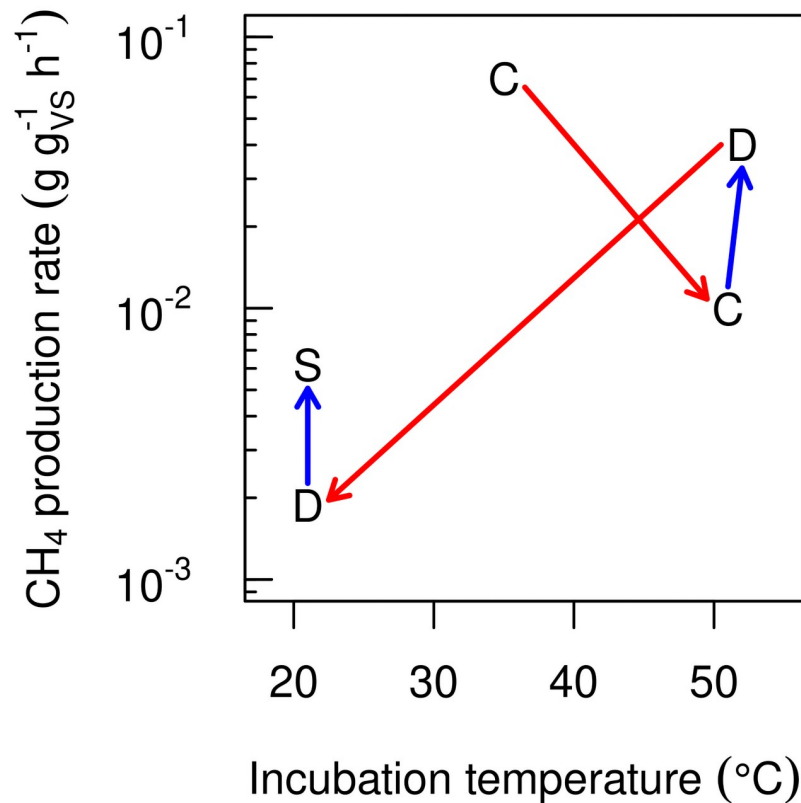


**Fig 1. Example of short- and long-term responses of methane production to temperature change.** Differences between short- and long-term response to temperature change measured by Elsgaard et al. [22]. Labels identify source: C = cattle manure (from barn), D = fresh digestate (directly from anaerobic digester), S = stored (> 1 month) digestate. Red arrows show short-term effects (differences between samples from the same source when incubated for 17 hours), and blue arrows apparent long-term effects (differences for samples stored for short and long time (weeks or months) at the same temperature)).

<https://doi.org/10.1371/journal.pone.0252881.g001>

changes in the temperature optimum of kinetic parameters for a single population of methanogens [27]. However, an empirical approach was used that does not explicitly represent the underlying mechanism. Gene sequencing has revealed that temperature changes shift the relative abundance of taxonomic groups of methanogens, indicating that changes in CH<sub>4</sub> production rates are due to selective growth of adapted methanogenic populations, rather than adaptation of an already established consortium [24, 28, 29]. Presumably the response to environmental stresses other than temperature also varies among methanogenic populations [30–32], and accordingly models need to include multiple groups of methanogens with different responses to temperature, and perhaps other stressors, in order to accurately predict both lag phases and the difference between short- and long-term response to changes in temperature and the chemical environment. This discussion also highlights an important challenge for prediction of CH<sub>4</sub> emission: measurements of short-term temperature responses in the laboratory, however careful, may not reflect long-term seasonal or geographic responses that are important for total CH<sub>4</sub> emissions.

Besides methanogens, there is evidence that sulfate reducing bacteria can affect CH<sub>4</sub> emission by competing for substrate (acetate or hydrogen) [33, 34], or by the production of inhibitory hydrogen sulfide (H<sub>2</sub>S) [35, 36]. This is particularly important for acidification of liquid manure with sulfuric acid, where prolonged suppression of CH<sub>4</sub> emission has been observed,

even when pH returned to or remained at near-neutral [15, 37]. In the absence of suitable electron acceptors, processes other than methanogenesis are not expected to play a major role beyond fermentation in this anaerobic environment [38]. Although sulfate may be used to oxidize ammonia [39], it is unlikely that this autotrophic process is important in organic-rich slurry. At the slurry-air interface, there is a potential for production of nitrous oxide ( $\text{N}_2\text{O}$ ) through nitrification and denitrification [40], as well as for bacterial methane oxidation [41, 42], but in both cases this depends on the development of a partly dry surface crust. While the model described below includes oxidation of organic matter in the surface layer, a crust represents a different environment that is outside the scope of the presented model. Still, these processes are part of a complete assessment of greenhouse gas emission from livestock operations.

Existing mechanistic models of organic matter degradation in anaerobic digesters describe biochemical pathways in detail, but are difficult to apply to highly variable manure environments due to lack of data. For example reported hydrolysis rate constants for slurry vary between  $0.004$  and  $0.13 \text{ d}^{-1}$  [43–45], possibly due to effects of feeding practice, manure management, or manure age [43, 46]. The main substrates for methanogenesis in slurry are volatile fatty acids (VFAs) and hydrogen [47, 48], but hydrogen is mainly derived from VFA oxidation [49, 50], and its regulatory role may be exaggerated [51]. Consequently, some models and simplified versions of detailed models merge hydrogen and VFA consumption kinetics to more simply represent organic matter degradation pathways [8, 11].

The considerations presented above strongly support the need for a new approach to predict  $\text{CH}_4$  emission from stored manure that describes both short- and long-term responses to management and storage conditions—including temperature and substrate availability—more accurately than current models. We propose that these responses can be accurately described using a simple dynamic model that includes multiple methanogenic populations with different temperature responses. Both inhibition and competition can easily be incorporated into this framework. The objective of the study was to develop and implement this approach as a new mechanistic model that can be used to better understand and predict of  $\text{CH}_4$  emission from slurry storage environments, including pits or channels inside barns and outside storage facilities.

## Methods

The new model presented in this paper predicts slurry organic matter transformation to  $\text{CH}_4$  using chemical oxygen demand (COD) as the base unit, though with conversion to a volatile solids (VS) basis for convenience. Carbon dioxide ( $\text{CO}_2$ ) production is also predicted, for a complete mass balance (or carbon balance) and also because it is a greenhouse gas. The essential model components are given below; further justification for these choices are presented in a related review [52].

1. Organic matter (volatile solids) includes three degradable components (particulate material, volatile fatty acids (VFAs), and microbial biomass) and a single non-degradable component, which is assumed to be completely conserved.
2. A single first-order expression for disintegration/hydrolysis and fermentation is used, reflecting the assumption that hydrolysis (but typically not fermentation) may limit the rate of  $\text{CH}_4$  production in slurry [43, 44, 53].
3. A Monod expression with VFAs as substrate is used for calculating microbial activity. This approach was chosen because Monod parameters are most frequently reported in the literature [11].

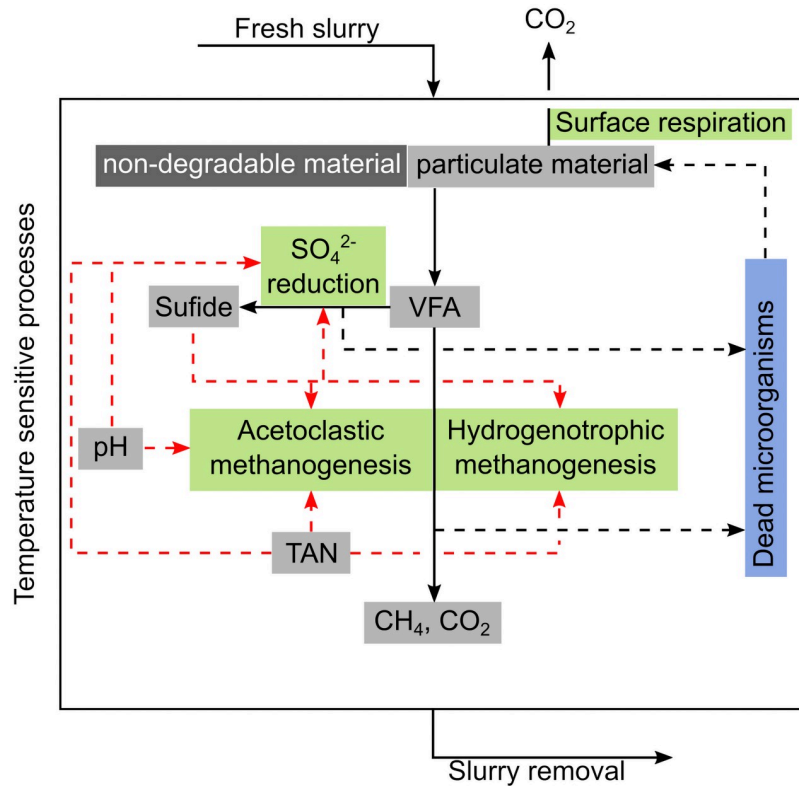


**Fig 2. Flow diagram of model concept.** Black lines indicate flows of organic matter, black dashed lines indicate flows of decayed microbial biomass. Red dashed lines indicate factors that inhibit microbial conversion processes (green boxes). Temperature affects all conversion processes, as well as chemical speciation.

<https://doi.org/10.1371/journal.pone.0252881.g002>

4. Multiple methanogen groups and one group of sulfate reducers, all with individual responses to temperature, are defined in order to capture microbial dynamics and short- and long-term changes in activity in response to temperature changes.
5. Management options that control slurry production- and removal rates are integrated to account for microbial adaptation in outside storages or in-house pits or channels.
6. Microbial inhibition factors are included for pH, free ammonia (NH<sub>3</sub> (aq)) and ammonium (NH<sub>4</sub><sup>+</sup>), and hydrogen sulfide (H<sub>2</sub>S).

### Model processes and algorithms

A flow diagram of the key processes included in the model are shown in Fig 2, and Table 1 summarizes processes and rates expressions.

Disintegration and hydrolysis of particulate material are considered rate limiting for subsequent degradation. Hence, combined disintegration, hydrolysis, and fermentation of degradable particulate material to VFAs is calculated with first order kinetics [43–45] (Eq 1).

$$\frac{dS_p}{dt} = -\alpha \cdot S_p - R + \sum_{i=1}^k (k_{d,i} \cdot X_i) + F_{in} \cdot C_{S_p,in} \quad (1)$$

In Eq 1,  $\alpha$  is the first-order rate constant (d<sup>-1</sup>),  $S_p$  is degradable particulate material in units of substrate COD (g<sub>COD-S</sub>), and  $t$  is time (d). Surface respiration rate,  $R$  (g<sub>COD-S</sub> m<sup>-2</sup> d<sup>-1</sup>),

**Table 1. Petersen matrix of model state variables (following [61], based on [62]).** See S3 Appendix for parameter descriptions and default values.

Component → j	1	2	3	4	5	6	7	8	Rate expression
<b>i Process ↓<sup>c</sup></b>	<b>S<sub>p</sub></b>	<b>VFAs</b>	<b>SO<sub>4</sub><sup>2-</sup></b>	<b>sulfide</b>	<b>CH<sub>4</sub></b>	<b>CO<sub>2</sub></b>	<b>X<sub>i</sub></b>	<b>X<sub>sr</sub></b>	
1 Hydrolysis & fermentation	-1	1							$\alpha \cdot S_p$
2 Methanogenesis of X <sub>i</sub> <sup>a</sup>		-1			$P_{CH_4}$	$P_{CO_2, anaer}$	$Y_i$		$\frac{q_{max} \cdot C_{VFA}}{K_S + C_{VFA}} \cdot X_i \cdot I_i$
3 Sulfate reduction of X <sub>sr</sub> <sup>a</sup>		-1	$f_{COD-S, sulfur}$	$f_{COD-S, sulfur}$		$P_{CO_2, sr}$		$Y_{sr}$	$\frac{q_{max} \cdot C_{VFA}}{K_S + C_{VFA}} \cdot \frac{C_{SO_4}}{K_{S,SO_4} + C_{SO_4}} \cdot X_{sr} \cdot I_{sr}$
4 Surface respiration	-1					$P_{CO_2, aer}$			$k_{L,O_2} \cdot area \cdot (0.208k_{H_2O_2} - 0)$
5 Hydrogen sulfide emission				-1					$kL_{H_2S} \cdot area \cdot (C_{H_2S} - 0)$
6 Decay of X <sub>i</sub> <sup>a</sup>	1						-1		$k_{d,i} \cdot X_i$
7 Decay of X <sub>sr</sub> <sup>a</sup>	1							-1	$k_{d,sr} \cdot X_{sr}$
8 Slurry addition	$F_{in}$	$F_{in}$	$F_{in}$	$F_{in}$	$F_{in}$		$F_{in}$	$F_{in}$	$C_{Si,in}$ or $C_{Xi,in}$
	Degradable organic matter (g <sub>COD-S</sub> )	Volatile fatty acids (g <sub>COD-S</sub> )	Sulfate (g <sub>SO<sub>4</sub>-sulfur</sub> )	Sulfide (g <sub>H<sub>2</sub>S-sulfur</sub> )	Methane (g <sub>CH<sub>4</sub></sub> )	Carbon dioxide (g <sub>CO<sub>2</sub></sub> )	Methanogen populations (g <sub>COD-B</sub> )	Sulfate reducer populations (g <sub>COD-B</sub> )	rate units i = 1–4 (g <sub>COD-S</sub> d <sup>-1</sup> ) i = 5 (g <sub>H<sub>2</sub>S-sulfur</sub> d <sup>-1</sup> ) i = 6,7 (g <sub>COD-B</sub> d <sup>-1</sup> ) i = 8 (g <sub>COD-S</sub> , g <sub>COD-B</sub> , g <sub>H<sub>2</sub>S-S</sub> , g <sub>SO<sub>4</sub>-S</sub> , g <sub>TAN</sub> ) d <sup>-1</sup>

<sup>a</sup> Can represent any number of microbial groups.

<sup>b</sup> Unit conversion factor.

<sup>c</sup> Slurry and components removal are not included in this table since these do not occur by rate. Instead see Eqs 8–11.

<https://doi.org/10.1371/journal.pone.0252881.t001>

reduces  $S_p$  but model predictions suggest it is only significant when the slurry depth is a few mm. Dead microbial biomass from any defined microbial group ( $i$ ) is reintroduced as  $S_p$ , where  $k_{d,i}$  (d<sup>-1</sup>) is the decay rate constant of the microbial groups.  $X_i$  represents the active biomass (g<sub>COD-B</sub>) of microbial group  $i$ , with a total of  $k$  groups, all methanogens except for 1 sulfate reducer.  $F_{in}$  is the slurry production rate (kg<sub>slurry</sub> d<sup>-1</sup>), and  $C_{Sp,in}$  is the  $S_p$  concentration of the introduced slurry (g<sub>COD-S</sub> kg<sub>slurry</sub><sup>-1</sup>). Hydrolysis of  $S_p$  yields VFAs (g<sub>COD-S</sub>), which in turn is consumed by microbial groups (Eq 2).

$$\frac{dVFA}{dt} = \alpha \cdot S_p - \sum_{i=1}^k r_i + F_{in} \cdot C_{VFA,in} \tag{2}$$

Here,  $r_i$  is the VFA utilization rate (g<sub>COD-S</sub> d<sup>-1</sup>), which follows Monod kinetics, and  $C_{VFA,in}$  is the VFA concentration (g<sub>COD-S</sub> kg<sub>slurry</sub><sup>-1</sup>) in the introduced slurry. The VFA utilization rate of each methanogen group  $r_i$  is linked to the active biomass (Eq 3) [38].

$$r_i = -\frac{q_{max,i} \cdot C_{VFA}}{K_{S,i} + C_{VFA}} \cdot X_i \cdot \prod_{j=1}^4 I_{i,j} \tag{3}$$

Here  $q_{max}$  is the temperature-dependent maximum specific substrate utilization rate (g<sub>COD-S</sub> g<sub>COD-B</sub><sup>-1</sup> d<sup>-1</sup>),  $K_S$  is the half-saturation constant (g<sub>COD-S</sub> kg<sub>slurry</sub><sup>-1</sup>), and  $C_{VFA}$  is the concentration of VFAs in the slurry (g<sub>COD-S</sub> kg<sub>slurry</sub><sup>-1</sup>), and  $X_i$  represents the active methanogen biomass of group  $i$ .  $I_{i,j}$  is a dimensionless inhibition term with a value between 0 and 1 that represents the sensitivity of group  $i$  to inhibitor  $j$  with a total of 4 potential inhibitors (Table 2).

Table 2. Equations used for inhibition factors.

Inhibition factor	Expression	Description	Reference
$I_{NH_3}$	$\begin{cases} 1, & C_{NH_3} \leq KI_{NH_3,min} \\ e^{-2.77259 \cdot \left( \frac{C_{NH_3} - KI_{NH_3,min}}{KI_{NH_3,max} - KI_{NH_3,min}} \right)^2}, & C_{NH_3} > KI_{NH_3,min} \end{cases}$	Inhibition factor for ammonia, where $KI_{NH_3,min}$ and $KI_{NH_3,max}$ are the $NH_3$ concentration at which inhibition starts and reach maximum, respectively	[63]
$I_{NH_4}$	$\begin{cases} 1, & C_{NH_4} \leq KI_{NH_4,min} \\ e^{-2.77259 \cdot \left( \frac{C_{NH_4} - KI_{NH_4,min}}{KI_{NH_4,max} - KI_{NH_4,min}} \right)^2}, & C_{NH_4} > KI_{NH_4,min} \end{cases}$	Inhibition factor for ammonium, where $KI_{NH_4,min}$ and $KI_{NH_4,max}$ are the $NH_4^+$ concentrations at which inhibition starts and reach 100% inhibition, respectively	[63]
$I_{pH}$	$\frac{1+2 \cdot 10^{0.5(pH_U - pH_L)}}{1+10^{(pH - pH_U)} + 10^{(pH_L - pH)}}$	Inhibition factor for pH, with upper ( $pH_U$ ) and lower ( $pH_L$ ) pH limits at which 50% inhibition occurs.	[8]
$I_{H_2S}$	$\begin{cases} 1 - \frac{C_{H_2S}}{KI_{H_2S}}, & C_{H_2S} \leq KI_{H_2S} \\ 0, & C_{H_2S} > KI_{H_2S} \end{cases}$	Inhibition factor for $H_2S$ , where $KI_{H_2S}$ is the $H_2S$ concentration at which 100% inhibition occurs.	[36]
$I$	$I_{NH_3} \cdot I_{NH_4} \cdot I_{pH} \cdot I_{H_2S}$	Joint inhibition factor	[11]

<https://doi.org/10.1371/journal.pone.0252881.t002>

The substrate utilization rate for sulfate reducers,  $r_{sr}$ , follows a double Monod expression (Eq 4) [36].

$$r_{sr} = -\frac{q_{max} \cdot C_{VFA}}{K_S + C_{VFA}} \cdot \frac{C_{SO_4}}{K_{S,SO_4} + C_{SO_4}} X_{sr} \cdot \prod_{j=1}^4 I_{sr,j} \tag{4}$$

where  $C_{SO_4}$  and  $K_{S,SO_4}$  are the concentration of  $SO_4^{2-}$  ( $g_{SO_4-S} \text{ kg}_{slurry}^{-1}$ ) and the half-maximum  $SO_4^{2-}$  saturation constant ( $g_{SO_4-S} \text{ kg}_{slurry}^{-1}$ ), respectively. (Note that charges on chemical species are omitted in subscripts for clarity in text and tables, e.g.,  $SO_4$  for sulfate.)  $X_{sr}$  represents the biomass of active sulfate reducing bacteria. Sulfate is reduced to sulfide in a 1:1 molar ratio, and loss of  $H_2S$  to the air is proportional to the slurry surface area ( $A$ ). Microbial growth of any group is linked to  $r_i$  through the biomass/substrate yield coefficient  $Y_i$  ( $g_{COD-B} \text{ g}_{COD-S}^{-1}$ ), and the biomass decay follows first order kinetics (Eq 5).

$$\frac{dX_i}{dt} = Y_i \cdot r_i - k_{d,i} \cdot X_i + F_{in} \cdot C_{X_i,in} \tag{5}$$

$C_{X_i,in}$  is the concentration of active microbial biomass ( $g_{COD-B} \text{ kg}_{slurry}^{-1}$ ) in the fresh slurry. Methane production is linked to substrate utilization  $r$  for methanogens using a  $CH_4$  productivity coefficient,  $P_{CH_4}$  ( $g_{CH_4} \text{ g}_{COD-S}^{-1}$ ), so  $CH_4$  production rate ( $g_{CH_4} \text{ d}^{-1}$ ) is given by Eq 6.

$$\frac{dCH_4}{dt} = P_{CH_4} \cdot \sum_{i=1}^{k-1} r_i \tag{6}$$

The  $CO_2$  production is linked to microbial activity through productivity coefficients ( $g_{CO_2} \text{ g}_{COD-S}^{-1}$ ) in Eq 7.

$$\frac{dCO_2}{dt} = P_{CO_2,anaerobic} \cdot \sum_{i=1}^{k-1} r_i + P_{CO_2,sr} \cdot r_{sr} + P_{CO_2,aerobic} \cdot R \tag{7}$$

Because  $P_{CO_2,anaerobic}$  includes  $CO_2$  from both fermentation and methanogenesis, it is only accurate when the system is in steady state, or as a cumulative response, and less so during VFA accumulation.

Slurry is added at a constant rate until the storage reaches maximum capacity (Eq 8), at which time slurry is removed, resulting in a new level (Eq 9).

$$\frac{dM_m}{dt} = F_{in} \tag{8}$$

$$M'_m = M_m \cdot f_{resid} \tag{9}$$

Slurry removal is instantaneous and occurs exactly when slurry mass  $M_m$  equals  $M_{m,max}$ .  $M'_m$  is the slurry mass after removal, and  $f_{resid}$  is the fraction of slurry retained in the channel after removal. The total mass of  $S_p$ , VFAs,  $SO_4^{2-}$ , TAN, and  $H_2S$  are similarly reduced.

Methanogen enrichment in residual slurry is probable in the light of documentation that methanogenic biofilms form on various materials under a range of environmental conditions [54–56]. To account for this, a microbial enrichment factor  $a_{enrich}$ , representing the increase in the odds of retention for a single microorganism relative to the odds for conservative components, was used (Eqs 10 and 11). An  $a_{enrich}$  value of zero implies no enrichment.

$$f_{resid,Xi} = \frac{e^{\ln\left(\frac{f_{resid}}{1-f_{resid}}\right) + a_{enrich}}}{1 + e^{\ln\left(\frac{f_{resid}}{1-f_{resid}}\right) + a_{enrich}}} \tag{10}$$

$$X'_i = X_i \cdot f_{resid,Xi} \tag{11}$$

Here,  $f_{resid,Xi}$  is the fraction of a single population retained after slurry removal and  $X'_i$  is the microbial biomass (g<sub>COD-B</sub>) of this group after slurry removal.

Temperature sensitivity of  $q_{max}$  and  $\alpha$  is based on the Cardinal Temperature Model (CTM1) [57, 58] shown for  $q_{max}$  in Eq 12.

$$q_{max} = q_{max,opt} \frac{(T - T_{max}) \cdot (T - T_{min})^2}{(T_{opt} - T_{min}) \cdot [(T_{opt} - T_{min}) \cdot (T - T_{opt}) - (T_{opt} - T_{max}) \cdot (T_{opt} + T_{min} - 2 \cdot T)]} \tag{12}$$

$q_{max}$  is calculated for each microbial population (group) by selecting the following temperature constraints on substrate utilization; minimum temperature of substrate utilization,  $T_{min}$  (°C), maximum temperature of substrate utilization,  $T_{max}$  (°C), the optimum temperature of substrate utilization,  $T_{opt}$  (°C), the temperature of the slurry material,  $T$  (°C), and the maximum substrate utilization rate at  $T_{opt}$ ,  $q_{max,opt}$  (g<sub>COD-S</sub> g<sub>COD-B</sub><sup>-1</sup> d<sup>-1</sup>). Traditionally, temperature effects on metabolic processes are described with a double Arrhenius expression [59]. The CTM1 model predicts a similar response and uses intuitive temperature inputs ( $T_{max}$ ,  $T_{min}$ ,  $T_{opt}$  and  $T$ ), which allows for easy tuning of microbial growth characteristics.  $K_S$  decreases with temperature according to an exponential function [60] (Eq 13).

$$K_S = K_{S,coef} \cdot k_1 \exp(-k_2 \cdot T) \tag{13}$$

The processes described above all affect state variables of the model, which are summarized in Table 1. Growth inhibition factors are presented in S2 Appendix. Temperature-dependent equations describing chemical speciation and air-slurry transfer of  $H_2S$  and  $O_2$  are provided in S2 Appendix.

### Methanogenic groups

The proposed model can accept any number of methanogenic groups, but for simplicity it should include only those necessary for reproducing important short- and long-term



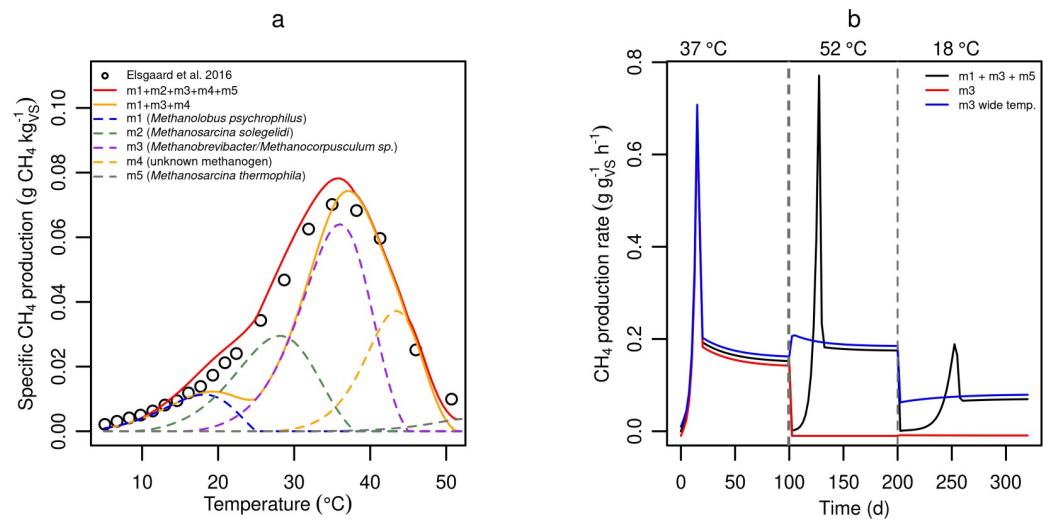


**Fig 3. Number of methanogen groups.** (a) Predicted  $\text{CH}_4$  production of single (dashed colored lines) and multiple (solid lines) methanogen groups as compared to observed  $\text{CH}_4$  production in cattle slurry by Elsgaard et al 2016 (circles). (b) Predicted short- and long-term responses to temperature change for different sets of methanogen groups. Note: Lines are shifted up or down by 0.01 for clarity.

<https://doi.org/10.1371/journal.pone.0252881.g003>

responses. Although this set may vary with application [31, 64], here we present a generic set based on the short-term temperature response for cattle manure presented by Elsgaard et al. [22], along with pure culture results from Jabłoński et al. [65]. Elsgaard et al. [22] studied  $\text{CH}_4$  production rates from slurry and digestate during incubation for up to two days at temperatures between 5 and 52°C and found methanogenic activity over the whole temperature range. Considering that the average temperature growth interval of methanogenic species in the database compiled by Jabłoński et al. [65] is only 25°C ( $n = 104$ ), observation of  $\text{CH}_4$  production over 47°C by Elsgaard et al. [22] suggest that multiple methanogen groups were present and active in the manure materials. Fig 3a shows the increased modelling accuracy achieved with multiple methanogen groups using temperature response profiles selected based on methanogenic community analysis studies of cattle slurry [48, 64, 66–68] and the methanogenic database [65]. At least five groups (red full line, with default parameter values for m1, m2, m3, m4, and m5) are required to match measured  $\text{CH}_4$  production over the whole temperature range. Thus, five groups that approximately represent individual methanogen species (with the exception of m4) were selected as the default set.

Although a single methanogen group could probably capture observed short-term responses, it is necessary to include multiple groups of methanogens to account for general differences between short- and long-term measurements (e.g., Fig 1). In Fig 3b the differences between a single and multiple methanogen groups in terms of short- and long-term effects are clearly demonstrated. The expected difference between short- and long-term responses is achieved only with multiple groups (black, with default parameter values for m1, m3, and m5). A single methanogen group, even with an extremely wide temperature growth interval, shows only minor differences in short vs long-term effects on  $\text{CH}_4$  production after a temperature change. On the other hand, with multiple methanogenic groups there is a large difference, where the short-term effect is a drop of  $\text{CH}_4$  emission followed by an increase and stabilization period in the long-term. This response is consistent with observations in multiple experiments [5, 14–17, 69] and confirms the importance of including multiple methanogen groups for accurate modelling of  $\text{CH}_4$  emission of slurry storage systems.

## Model parameters

Based on Fig 3, five methanogen groups (m1—m5) were chosen as default. Temperature optima of these groups are based on individual species: *Methanobrevibacter* (m1), *Metahnosarcina solegelid* (m2), *Metahnobrevibacter*/*Methanocorpusculum* sp. (m3), and *Methanosarcina thermophilia* (m5). The final group (m4) is not based on a known species, but instead has an optimum temperature equidistant between that of m3 and m5. The  $q_{max,opt}$  of each group was calculated from its optimum growth temperature shown in Fig 4a, by assuming a linear increase from 0  $\text{g}_{\text{COD-S}} \text{g}_{\text{COD-B}}^{-1} \text{d}^{-1}$  at 0°C to 8  $\text{g}_{\text{COD-S}} \text{g}_{\text{COD-B}}^{-1} \text{d}^{-1}$  at 40°C. In comparison, by default ADM1 uses 8  $\text{g}_{\text{COD-S}} \text{g}_{\text{COD-B}}^{-1} \text{d}^{-1}$  at 35°C [11]. The temperature dependent  $q_{max}$  for individual populations (Fig 3a) is calculated using  $q_{max,opt}$  according to Eq 12. For all methanogen groups, biomass yield  $Y_i$  was fixed at 0.05  $\text{g}_{\text{COD-B}} \text{g}_{\text{COD-S}}^{-1}$ , equal to the recommended value for acetoclastic methanogen in ADM1 [10] and the mean value from the literature review presented by Weinrich [70, 71] ( $n = 37$  measurements). The  $q_{max,opt}$  and  $Y_i$  of the optional sulfate reducer group, sr1, were calculated based on the relative  $q_{max,opt}$  and  $Y_i$  difference between typical acetoclastic methanogens and acetoclastic sulfate reducers [38]. Hydrogenotrophic methanogens such as *Methanobrevibacter* and *Methanocorpusculum* (m3) are highly abundant in fresh manure and in the animal intestinal tract [48, 65, 72, 73], and hence the m3 active biomass concentration in the produced slurry is by default an order of magnitude greater than for any other methanogen group (0.01 vs 0.001  $\text{g}_{\text{COD-B}} \text{kg}_{\text{Slurry}}^{-1}$ ). The  $K_s$  was calculated using Eq 13, where  $K_{s,coef}$  by default is 1, but can be modified for individual microbial groups to reflect differences in substrate affinity for e.g. acetoclastic methanogens, hydrogenotrophic methanogens [74–76] and sulfate reducers [33, 34]. For the same reasons, inhibition constants can be specified for individual microbial groups [36, 77]. The temperature dependent disintegration/hydrolysis/fermentation rate constant,  $\alpha$ , was calculated from Eq 12 with default  $\alpha_{opt} = 0.02 \text{ d}^{-1}$  at  $T_{opt} = 50$ ,  $T_{min} = 0$ , and  $T_{max} = 60$ °C. Productivity coefficients for  $\text{CH}_4$  and  $\text{CO}_2$  were calculated based on microbial stoichiometry (see S1 Appendix) [38, 78]. The default value of a mass transfer coefficient for  $\text{O}_2$  was based on respiration rates measured by Markfoged [79], and for  $\text{H}_2\text{S}$ , was estimated by assuming depletion occurred

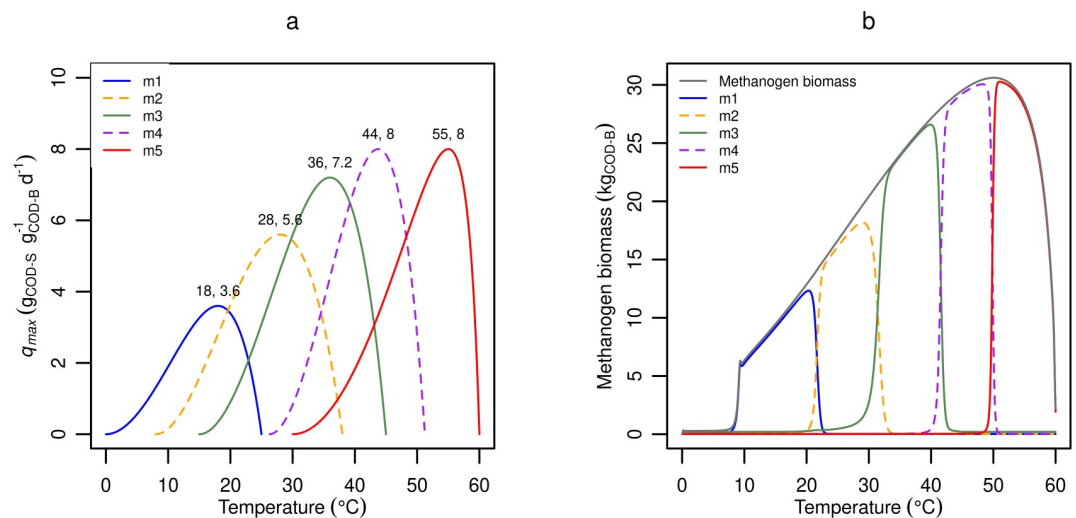


**Fig 4. Default temperature responses.** (a) Temperature dependence of maximum substrate utilization rates ( $q_{max}$ ) of default methanogen groups in the model (m1 to m5). (b) Steady-state microbial biomass as a function of temperature for default parameter values. The residual fraction of slurry ( $f_{resid}$ ) was set to 0.95 in this simulation.

<https://doi.org/10.1371/journal.pone.0252881.g004>

within a 1 cm film at the surface. The complete list of default parameter values and input variables are found in [S3 Appendix](#).

[Fig 4b](#) shows the model-predicted steady state abundance of the default microbial groups as a function of temperature. The steady state active methanogen biomass smoothly increases with temperature above about 10°C, despite shifting dominance among methanogen groups. This correlation is an indirect consequence of higher  $q_{max}$  and  $\alpha$  with increasing temperature. However, low  $q_{max}$  below 10°C translates into very limited growth of m1, which is consistent with small CH<sub>4</sub> emissions reported at low temperatures [6, 22]. Above 10°C the total methanogen biomass curve resembles the shape of the hydrolysis rate curve ([Eq 12](#)), because hydrolysis (i.e., substrate availability and not maximum methanogen growth rates) is rate limiting in this simulation, due to the emptying interval and residual fraction (see “Model behavior” section).

### Model behavior and application

The model was implemented in the R language [80] as a function, and is available as an add-on package from GitHub at <https://github.com/sashahafner/ABM>. A vignette included with the package provides an introduction to the use of the model. The `abm()` function in this package (version 1.18.0) was used to generate results shown in this work.

Effects of slurry retention time, temperature change, and pH were explored in order to show the behavior of the model. Simulations were generally run using the default parameter settings, with a slurry production rate of 1000 kg d<sup>-1</sup> and a slurry storage capacity of 33333 kg, equivalent to conditions of a slurry channel or pit receiving fresh excreta, and being emptied (except for a 10% residual fraction) every 30 days. The default temperature is 20°C and pH is 7. Below, deviations from default parameters are explicitly stated and listed in [S3 Appendix](#). In addition, we present a sensitivity analysis, and a comparison of model simulations to measurements from a farm scale experiment. To show the capability of the model to describe CH<sub>4</sub> emissions from real livestock production facilities, we compared model simulations to data from Kariyapperuma et al. [6], who measured CH<sub>4</sub> emission from an outside slurry storage tank with a maximum capacity of about 2700 m<sup>3</sup>. The slurry storage tank periodically received manure from a pre-storage underneath a barn with approximately 200 cows. For additional details on the manure management see [6]. The dataset lacked information about the initial and subsequently introduced slurry composition, and instead we made qualified guesses and ran multiple simulation scenarios to assess model performance. The dataset included time series of organic matter concentration in units of VS, and hence conversion to degradable particulate material (COD units) was needed to make it compatible with the model input unit. Since COD measurement is error-prone for particulate materials [81], use of a conversion factor to estimate COD from VS is preferable to direct measurement. The degradable fraction of VS ( $VS_d$ ) in cattle slurry was set to 0.42, based on the average of two studies [82, 83]. The COD-to-VS ratio was estimated at 1.42 g<sub>COD-S</sub>/g<sub>VS</sub> for cattle slurry based on average slurry composition [82] and calculated oxygen demand [38] ([S1 Appendix](#)). We assumed that half the  $VS_d$  had been degraded at the start of the measurements, based on recent estimates suggesting that 28% of  $VS_d$  in cattle slurry from barns is consumed over a collection period of 30 days [84], and the much longer retention time in Kariyapperuma [6]. The model inputs for the simulation are provided in [S4 Appendix](#). Measured temperature and slurry mass data were linearly interpolated to provide daily values for simulations. The dataset consisted of seasonal campaigns with daily measurements of temperature and slurry mass during two years. Gap-filling to obtain a complete dataset covering 730 days was done by referring to corresponding data from a second measurement year (e.g., because temperature data was missing for spring 2010, we used measurements from spring 2011) ([S4 Appendix](#)). This extended dataset was

used as model input, and then CH<sub>4</sub> emission was simulated for five consecutive 730-day periods to ensure stable predictions. The fifth simulation round was compared to CH<sub>4</sub> emissions measured by Kariyapperuma et al. [6].

## Results and discussion

### Model behavior

In this section effects of residual slurry and methanogen enrichment, temperature changes, and pH on predicted CH<sub>4</sub> production are presented in order to show the behavior of the model.

**Residual fraction and methanogen enrichment.** The residual fraction of slurry after export and the enrichment of active methanogens in the residue are expected to enhance methane production from fresh excreta. Fig 5 shows predicted effects of varying the residual fraction of slurry between 1 and 50% with or without enrichment of methanogens in the residue. Total methanogen biomass (Fig 5a) and CH<sub>4</sub> production (Fig 5b) were correlated, and both quantities were substantially reduced when the slurry channel was emptied to 0.5% ( $f_{resid} = 0.005$ ) as compared to 10% or 50% ( $f_{resid} = 0.1$  or 0.5). The differences could be partially explained by the average amount of slurry in the tank, but was primarily a result of the smaller methanogen population being retained when the residual slurry fraction was low. Changing the microbial enrichment factor ( $a_{enrich}$ ) significantly impacted methanogen biomass only for the lowest residual fraction  $f_{resid} = 0.005$ . At  $f_{resid} = 0.5$ , and  $f_{enrich} = 5$ , methanogen retention was effectively close to 100%, resulting in complete consumption of available VFAs, and hydrolysis limiting CH<sub>4</sub> production, which explains why CH<sub>4</sub> production was almost identical for  $f_{enrich} = 5$  and 0. Altogether, the results in Fig 5 demonstrate that a substantial CH<sub>4</sub> reduction can be expected by near-complete emptying of the slurry channel.

**Temperature effects.** The implementation of temperature sensitive methanogen groups allowed for simulating effects of gradual (seasonal) temperature changes, as well as transient and prolonged effects of rapid temperature change (i.e. slurry export from a barn to an outside storage, or from the animal tract to a slurry channel or pit). Fig 6a shows methanogen groups

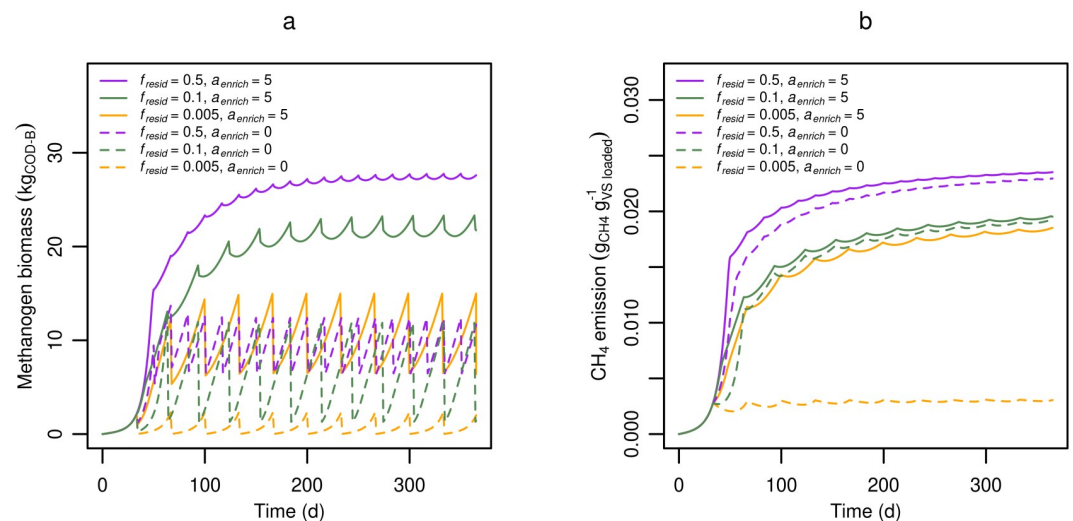


**Fig 5. Predicted effects of residual slurry fraction on methanogens and methane production.** (a) Total methanogen biomass and (b) Cumulative CH<sub>4</sub> emission as affected by the residual fraction ( $f_{resid}$ ) of slurry after slurry removal assuming a high degree of microbial enrichment ( $a_{enrich}$ ), or no enrichment.

<https://doi.org/10.1371/journal.pone.0252881.g005>

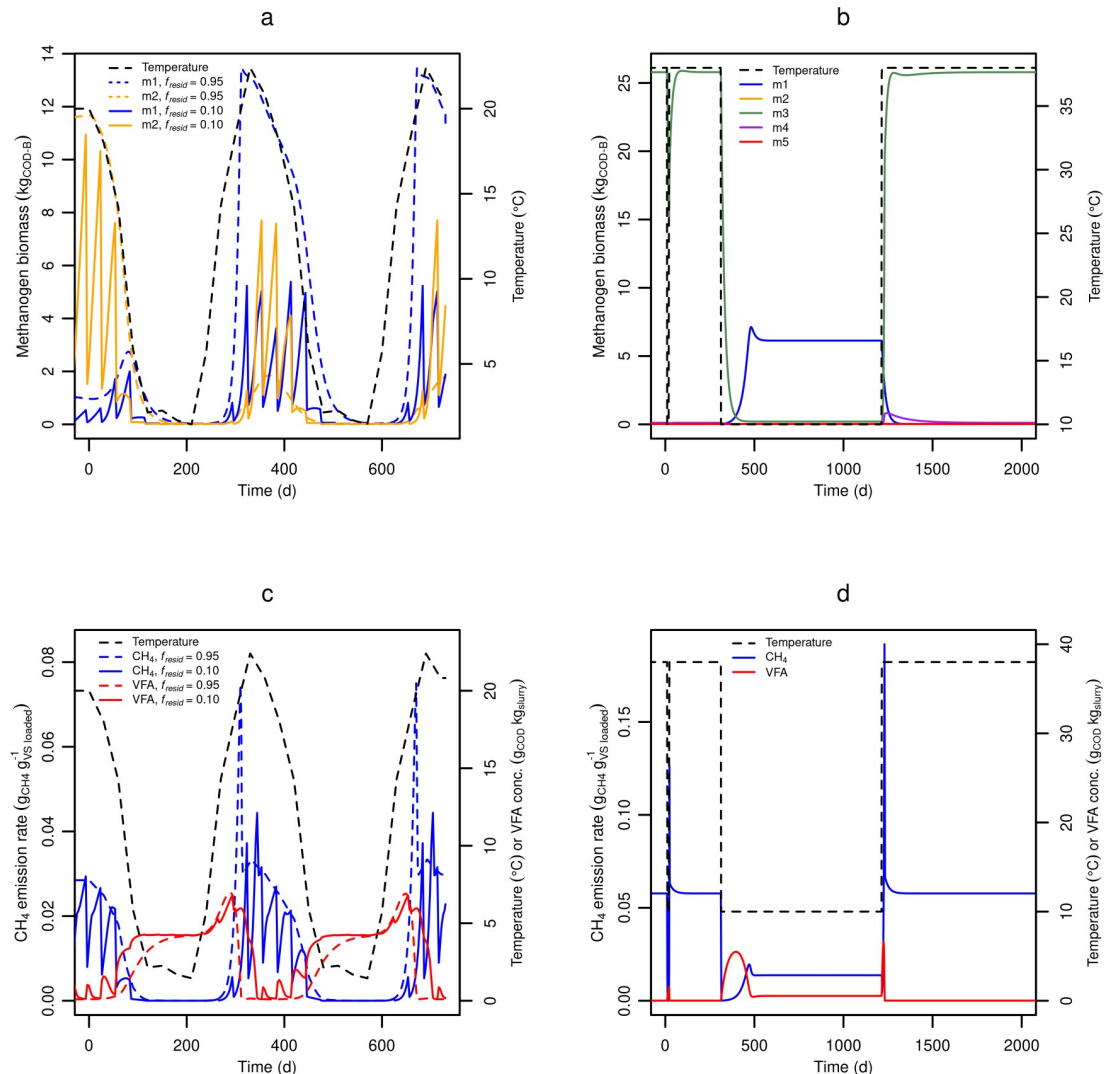


**Fig 6. Predicted temperature effects on methanogens and methane production.** (a) Methanogen biomass and (c) CH<sub>4</sub> emission during gradual slurry temperature changes as predicted with a high and low residual slurry fraction in the storage ( $f_{resid}$ ). (b) Methanogen biomass and (d) CH<sub>4</sub> emission during short- and long-term temperature changes using a large residual fraction of slurry ( $f_{resid}$ ) of 0.95.

<https://doi.org/10.1371/journal.pone.0252881.g006>

responding to a seasonal change in slurry temperature (temperatures from Kariyapperuma et al. [6]). It was predicted that at high residual slurry fraction ( $f_{resid} = 0.95$ ) the methanogen biomass (Fig 6a) and CH<sub>4</sub> emission (Fig 6c) will peak when the temperature peaks, but the response to the temperature change was not immediate neither with increasing nor decreasing temperature. The delay reflects the time required for a change in microbial biomass. On the other hand, significant hysteresis was observed when the residual fraction was low ( $f_{resid} = 0.1$ ), with methanogen biomass and CH<sub>4</sub> emission peaking 1–2 months after the temperature. A similar delay was seen in Kariyapperuma et al. [6], where relatively large portions of manure were added and removed, similar to the use of a small residual fraction. In Fig 6c, a large CH<sub>4</sub> emission spike was predicted in response to increasing temperature, which reflects the rapid consumption of VFAs that had accumulated during the preceding cold period. This result reflects a low sensitivity of hydrolysis and fermentation to decreasing temperature in the

model, compared to methanogenesis, although in reality this dynamic may be more complex. However, the accumulation of VFAs after rapid temperature changes has been observed in multiple studies [24, 27, 85]. In Fig 6b and 6d the effects of an instantaneous temperature decrease lasting 10 or 300 days are shown. Methanogen numbers declined only slightly during a 10-day temperature decrease (Fig 6b), resulting in a significant CH<sub>4</sub> spike once the temperature was raised again (Fig 6d). In contrast, during a 900-day temperature decrease, m3 completely disappeared, resulting in a longer period of low CH<sub>4</sub> production when the temperature later increased. Concomitantly, while a surplus of VFA substrate was transiently available after the temperature increase (Fig 6d), m4 grew alongside m3, but as VFAs were depleted, m4 was outcompeted again. In reality both m3 and m4 may need to acclimatize to the environment before consuming VFAs, which in the model could be accounted for by implementing a lag phase where CH<sub>4</sub> production from a single methanogen population is temporarily halted in order to adjust cellular metabolism to new conditions, before resuming CH<sub>4</sub> production. This mechanism, however, seems very difficult to describe with equations relating to actual biochemical processes due to complexity and lack of knowledge about the lag phase [86].

The new model effectively assumes a linear temperature dependency of long-term CH<sub>4</sub> production rate (under non-limiting conditions), an assumption also made in other models [27, 51, 87]. However, for short-term dynamics of CH<sub>4</sub> emissions there is solid evidence for an Arrhenius-like temperature dependency of hydrolysis and methanogenesis [22, 45, 58], and the long-term link between temperature and CH<sub>4</sub> production rate remains to be studied systematically, particularly in the psychrophilic temperature range where slurry is often stored.

**Acidification.** Acidification to suppress ammonia volatilization has been shown to reduce CH<sub>4</sub> emissions from cattle and pig slurry by 70–90% [15, 31, 37]. Fig 7 shows the predicted response to an instantaneous drop in pH, as in acidification in a storage tank. The immediate reduction in pH resulted in net microbial decay (Fig 7a) while immediately reducing CH<sub>4</sub> emissions (Fig 7b). The apparent dominance of the m3 group during low pH was a consequence of its naturally higher abundance in the fresh slurry that was added each day. Once pH increased, the methanogens recovered and CH<sub>4</sub> emissions rose again. However, in practical slurry management systems, the pH drop is typically achieved by sulfuric acid treatment, which inevitably raises the SO<sub>4</sub><sup>2-</sup> concentration to a level where sulfate reducing bacteria gain a thermodynamic advantage over methanogens. Therefore the model includes an optional

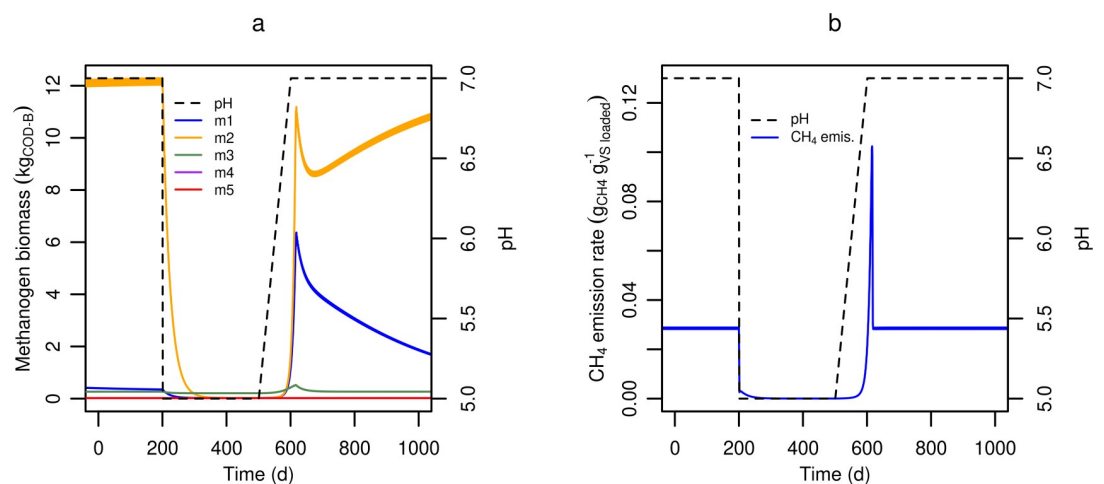


**Fig 7. Predicted pH effects on methanogens and methane production.** (a) Methanogen biomass and (b) CH<sub>4</sub> emission responses to pH changes. The residual fraction of slurry ( $f_{resid}$ ) was set to 0.95.

<https://doi.org/10.1371/journal.pone.0252881.g007>

sulfate reducer group (sr1) as demonstrated in [S5 Appendix](#). Inclusion of sr1 decreased the magnitude and delayed by several months the CH<sub>4</sub> peak after the pH was raised again. This response resulted primarily from increased competition between methanogen groups and sr1 for VFA substrate when SO<sub>4</sub><sup>2-</sup> was abundant, reflecting the known competition between the two groups [88]. A simulation with sr1 is probably more realistic for modelling acidification of slurry with sulfuric acid, but has the disadvantage of introducing additional parameters with associated uncertainty.

Similar to the effect of pH, the inhibiting effects of total ammoniacal nitrogen (TAN) and H<sub>2</sub>S were modelled by factoring a term directly onto the substrate utilization rate. An example of TAN inhibition is presented in [S6 Appendix](#).

### Sensitivity analysis

Cumulative CH<sub>4</sub> production was most sensitive to the hydrolysis rate constant parameter,  $\alpha_{opt}$  and the temperature input variable,  $T$  ([Fig 8a and 8b](#)). The model response is relatively insensitive to increases in the Monod parameters, but sensitive to decreases in the yield ( $Y_i$ ) and maximum substrate utilization rate ( $q_{max,opt}$ ). It is important to state that non-default parameters may significantly change model sensitivity to other parameters. Hydrolysis remains the least well-defined step in anaerobic digestion [43], and it can be considered the most critical input for the model performance. Significant effort should therefore be made to determine  $\alpha_{opt}$ .

### Model application

In [Fig 9](#) the model was applied to the case study of Kariyapperuma et al. [6] to show the qualitative responses of the model against real measurements. The simulation was run with different hydrolysis rates ([Fig 9a](#)), which resulted in CH<sub>4</sub> emission peaks of different magnitude, with  $\alpha_{opt} = 0.02$  matching best with measurements in terms of peak height. However, emissions were predicted to occur much too soon. The substrate utilization rate ( $q_{max,opt}$ ) was reduced, which postponed the CH<sub>4</sub> emission peaks to match better with data ([Fig 9b](#)). As suggested in [Fig 4b](#), methanogenesis is rate-limiting at low temperatures, explaining the observed effect of reducing  $q_{max,opt}$ . There is a need for model validation in controlled experiments, and

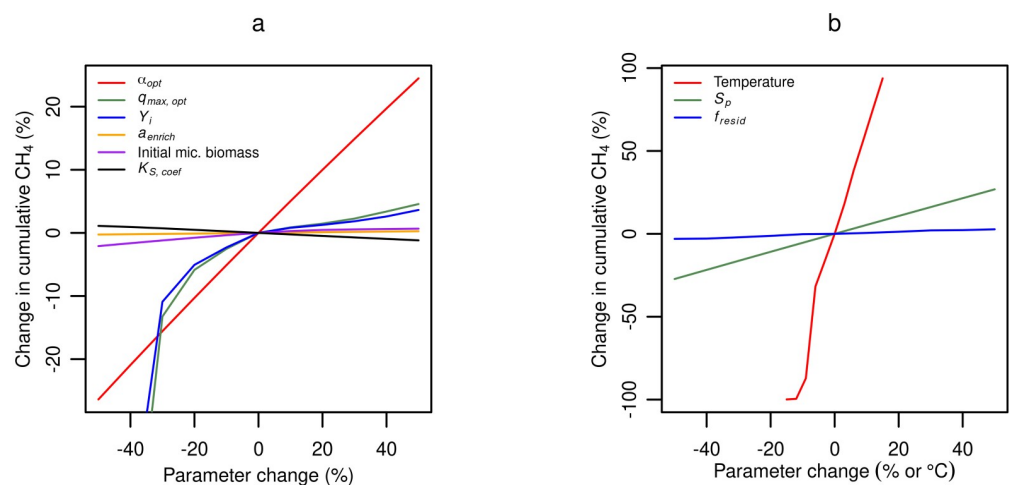


**Fig 8. Model sensitivity to parameters and input variables.** Model output sensitivities to (a) parameters and (b) input variables. Initial microbial biomass refers to changes in both the initial concentration of methanogens in the slurry inoculum and the fresh influent slurry. For parameter values, see [S3 Appendix](#).

<https://doi.org/10.1371/journal.pone.0252881.g008>

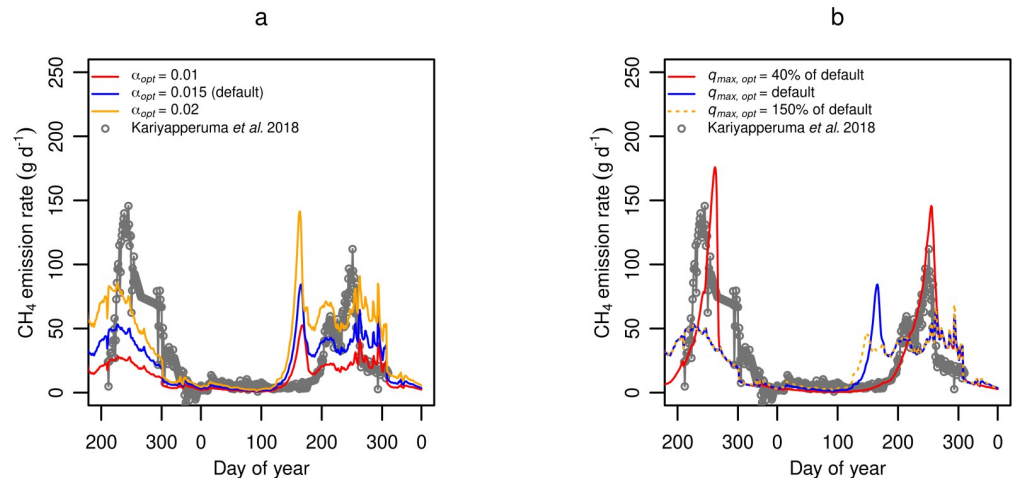


**Fig 9. Model application to case study.** Model results versus measured [6] CH<sub>4</sub> emission from a full scale slurry tank with periodic slurry introduction applying different (a) hydrolysis rates ( $\alpha_{opt}$ ) and (b) maximum substrate utilization rates at optimum temperature ( $q_{max,opt}$ ).

<https://doi.org/10.1371/journal.pone.0252881.g009>

with the necessary input data. The total concentration and relative fractions of degradable and slowly degradable particulate material can be measured [82], but this is rarely done. Furthermore, emission studies on full-scale storages often report only the composition of slurry in the storage and not information about the influent slurry composition [6, 89]. The new model presented here relies on characterization of the influent slurry composition to determine hydrolysis rate and CH<sub>4</sub> potential, and we stress therefore the importance of accurately measuring degradable particulate material and VFAs for accurate prediction of CH<sub>4</sub> emission.

## Conclusions

With multiple groups (populations) of methanogens, a mechanistic model of methane production from animal manure or similar wastes can reproduce complex observed responses to temperature, in particular, the distinctly different short- and long-term responses to temperature change. The new model described here, implemented in the ABM R package, is a flexible tool that can facilitate research on CH<sub>4</sub> emission and its control. Accounting for temporary inactivation of methanogens, methane oxidation, and possibly other processes may be necessary for the most accurate predictions, and model extension is possible. An application of the model to field data showed that detailed measurements of slurry organic matter composition will be needed for model extension and future application at all scales.

## Supporting information

**S1 Appendix. Assumptions about unit conversion and manure composition.** Explanation and numeric values for VS composition and conversion between VS and COD. (PDF)

**S2 Appendix. Additional model equations.** Additional equations used in the model not described in paper. (PDF)



**S3 Appendix. Parameters and variables.** Parameter and variable values used as defaults and in “Model behavior” section.

(PDF)

**S4 Appendix. Input data.** Input data used for simulating the conditions in the case study by Kariyapperuma et al. [6].

(PDF)

**S5 Appendix. Sulfate reducers and low pH.** Model predictions for the effect of acidification with inclusion of a sulfate reducer population.

(PDF)

**S6 Appendix. Ammonia inhibition dynamics.** Model predictions for ammonia inhibition of methanogens.

(PDF)

## Acknowledgments

We thank Associate Professor Anders Feilberg who provided the necessary facilities for completing the work.

## Author Contributions

**Conceptualization:** Frederik R. Dalby, Sasha D. Hafner, Søren O. Petersen, Kari Dunfield, Martin H. Chantigny, Sven G. Sommer.

**Data curation:** Frederik R. Dalby, Sasha D. Hafner, Søren O. Petersen, Andrew Vanderzaag.

**Formal analysis:** Frederik R. Dalby, Sasha D. Hafner, Søren O. Petersen.

**Investigation:** Frederik R. Dalby, Sasha D. Hafner, Jemaneh Habtewold, Sven G. Sommer.

**Methodology:** Frederik R. Dalby, Sasha D. Hafner, Sven G. Sommer.

**Project administration:** Sven G. Sommer.

**Resources:** Andrew Vanderzaag, Sven G. Sommer.

**Software:** Frederik R. Dalby, Sasha D. Hafner.

**Supervision:** Sasha D. Hafner, Søren O. Petersen, Andrew Vanderzaag, Sven G. Sommer.

**Validation:** Frederik R. Dalby, Sasha D. Hafner, Andrew Vanderzaag.

**Visualization:** Frederik R. Dalby, Sasha D. Hafner.

**Writing – original draft:** Frederik R. Dalby, Sasha D. Hafner.

**Writing – review & editing:** Frederik R. Dalby, Sasha D. Hafner, Søren O. Petersen, Andrew Vanderzaag, Jemaneh Habtewold, Kari Dunfield, Martin H. Chantigny, Sven G. Sommer.

## References

1. Jackson RB, Saunio M, Bousquet P, Canadell JG, Poulter B, Staver AR, et al. Increasing anthropogenic methane emissions arise equally from agricultural and fossil fuel sources. *Environmental Research Letters*. 2020; 15: 0–7. <https://doi.org/10.1088/1748-9326/ab9ed2>
2. FAO. Results | Global Livestock Environmental Assessment Model (GLEAM) | Food and Agriculture Organization of the United Nations. 2021 [cited 11 May 2021]. <http://www.fao.org/gleam/results/en/#c303615>

3. Dong H, MacDonald JD, Ogle SM, Sanz MJS, Rocha MT. Agriculture, Forestry and Other Land Use. 2019 Refinement to the 2006 IPCC Guidelines for National Greenhouse Gas Inventories. Ottawa, Canada: IPCC; 2019.
4. Mangino J, Bartram D, Brazy A. Development of a methane conversion factor to estimate emissions from animal waste lagoons. 11th International Emission Inventory Conference. 2001.
5. Baral KR, Jégo G, Amon B, Bol R, Chantigny MH, Olesen JE, et al. Greenhouse gas emissions during storage of manure and digestates: Key role of methane for prediction and mitigation. *Agricultural Systems*. 2018; 166: 26–35. <https://doi.org/10.1016/j.agsy.2018.07.009>
6. Kariyapperuma KA, Johannesson G, Maldaner L, VanderZaag A, Gordon R, Wagner-Riddle C. Year-round methane emissions from liquid dairy manure in a cold climate reveal hysteretic pattern. *Agricultural and Forest Meteorology*. 2018; 258: 56–65. <https://doi.org/10.1016/j.agrformet.2017.12.185>
7. Baldé H, VanderZaag AC, Burt S, Evans L, Wagner-Riddle C, Desjardins RL, et al. Measured versus modeled methane emissions from separated liquid dairy manure show large model underestimates. *Agriculture, Ecosystems & Environment*. 2016; 230: 261–270. <https://doi.org/10.1016/j.agee.2016.06.016>
8. Angelidaki I, Ellegaard L, Ahring BK. A mathematical model for dynamic simulation of anaerobic digestion of complex substrates: Focusing on ammonia inhibition. *Biotechnology and Bioengineering*. 1993; 42: 159–166. <https://doi.org/10.1002/bit.260420203> PMID: 18612976
9. Hill DT. A comprehensive dynamic model for animal waste methanogenesis. *Transactions of the ASAE*. 1982; 25: 1374–1380.
10. Batstone DJ, Keller J, Angelidaki I. Anaerobic digestion model no. 1. IWA publishing; 2002.
11. Batstone DJ, Keller J, Angelidaki I, Kalyuzhnyi S V., Pavlostathis SG, Rozzi A, et al. The IWA Anaerobic Digestion Model No 1 (ADM1). *Water science and technology: a journal of the International Association on Water Pollution Research*. 2002; 45: 65–73. <https://doi.org/10.2166/wst.2002.0292>
12. Batstone DJ, Puyol D, Flores-Alsina X, Rodríguez J. Mathematical modelling of anaerobic digestion processes: applications and future needs. *Rev Environ Sci Biotechnol*. 2015; 14: 595–613. <https://doi.org/10.1007/s11157-015-9376-4>
13. Wade MJ. Not Just Numbers: Mathematical Modelling and Its Contribution to Anaerobic Digestion Processes. *Processes*. 2020; 8: 888. <https://doi.org/10.3390/pr8080888>
14. Aguerre MJ, Wattiaux MA, Powell JM. Emissions of ammonia, nitrous oxide, methane, and carbon dioxide during storage of dairy cow manure as affected by dietary forage-to-concentrate ratio and crust formation. *Journal of Dairy Science*. 2012; 95: 7409–7416. <https://doi.org/10.3168/jds.2012-5340> PMID: 23021756
15. Petersen SO, Andersen AJ, Eriksen J. Effects of Cattle Slurry Acidification on Ammonia and Methane Evolution during Storage. *Journal of Environment Quality*. 2012; 41: 88. <https://doi.org/10.2134/jeq2011.0184> PMID: 22218177
16. Sommer SG, Clough TJ, Balaine N, Hafner SD, Cameron KC. Transformation of Organic Matter and the Emissions of Methane and Ammonia during Storage of Liquid Manure as Affected by Acidification. *Journal of Environmental Quality*. 2017; 46: 514–521. <https://doi.org/10.2134/jeq2016.10.0409> PMID: 28724090
17. Sokolov VK, VanderZaag A, Habtewold J, Dunfield K, Wagner-Riddle C, Venkiteswaran JJ, et al. Dairy manure acidification reduces CH<sub>4</sub> emissions over short and long-term. *Environmental Technology (United Kingdom)*. 2020; 0: 1–8. <https://doi.org/10.1080/09593330.2020.1714744> PMID: 31920167
18. Masse D, Masse L, Claveau S, Benchaar C, Thomas O. Methane emissions from manure storages. *Transactions of the ASABE*. 2008; 51: 1775–1781. Available: [http://apps.isiknowledge.com/full\\_record.do?product=WOS&search\\_mode=GeneralSearch&qid=27&SID=3D2i6D8f8e1@d46nfl&page=1&doc=2](http://apps.isiknowledge.com/full_record.do?product=WOS&search_mode=GeneralSearch&qid=27&SID=3D2i6D8f8e1@d46nfl&page=1&doc=2)
19. Wood JD, VanderZaag AC, Wagner-Riddle C, Smith EL, Gordon RJ. Gas emissions from liquid dairy manure: complete versus partial storage emptying. *Nutrient Cycling in Agroecosystems*. 2014; 99: 95–105. <https://doi.org/10.1007/s10705-014-9620-2>
20. Massé DI, Jarret G, Hassanat F, Benchaar C, Saady NMC. Effect of increasing levels of corn silage in an alfalfa-based dairy cow diet and of manure management practices on manure fugitive methane emissions. *Agriculture, Ecosystems & Environment*. 2016; 221: 109–114. <https://doi.org/10.1016/j.agee.2016.01.018>
21. Ngwabie NM, Gordon RJ, VanderZaag A, Dunfield K, Sissoko A, Wagner-Riddle C. The Extent of Manure Removal from Storages and Its Impact on Gaseous Emissions. *Journal of Environmental Quality*. 2016; 45: 2023–2029. <https://doi.org/10.2134/jeq2016.01.0004> PMID: 27898786

22. Elsgaard L, Olsen AB, Petersen SO. Temperature response of methane production in liquid manures and co-digestates. *Science of the Total Environment*. 2016; 539: 78–84. <https://doi.org/10.1016/j.scitotenv.2015.07.145> PMID: 26356180
23. Chen M. Adaptation of mesophilic anaerobic sewage fermentor populations to thermophilic temperatures. *Applied and Environmental Microbiology*. 1983; 45: 1271–1276. <https://doi.org/10.1128/aem.45.4.1271-1276.1983> PMID: 6859847
24. Lindorfer H, Waltenberger R, Köllner K, Braun R, Kirchmayr R. New data on temperature optimum and temperature changes in energy crop digesters. *Bioresource Technology*. 2008; 99: 7011–7019. <https://doi.org/10.1016/j.biortech.2008.01.034> PMID: 18343659
25. Ortega L, Barrington S, Guiot SR. Thermophilic adaptation of a mesophilic anaerobic sludge for food waste treatment. *Journal of Environmental Management*. 2008; 88: 517–525. <https://doi.org/10.1016/j.jenvman.2007.03.032> PMID: 17900789
26. Tian Z, Zhang Y, Li Y, Chi Y, Yang M. Rapid establishment of thermophilic anaerobic microbial community during the one-step startup of thermophilic anaerobic digestion from a mesophilic digester. *Water Research*. 2015; 69: 9–19. <https://doi.org/10.1016/j.watres.2014.11.001> PMID: 25463927
27. Kovalovszki A, Treu L, Ellegaard L, Luo G, Angelidaki I. Modeling temperature response in bioenergy production: Novel solution to a common challenge of anaerobic digestion. *Applied Energy*. 2020; 263: 114646. <https://doi.org/10.1016/j.apenergy.2020.114646>
28. Chachkhiani M, Dabert P, Abzianidze T, Partskhaladze G, Tsiklauri L, Dudaauri T, et al. 16S rDNA characterisation of bacterial and archaeal communities during start-up of anaerobic thermophilic digestion of cattle manure. *Bioresource Technology*. 2004; 93: 227–232. <https://doi.org/10.1016/j.biortech.2003.11.005> PMID: 15062816
29. Van Lier JB, Martin JLS, Lettinga G. Effect of temperature on the anaerobic thermophilic conversion of volatile fatty acids by dispersed and granular sludge. *Water Research*. 1996; 30: 199–207. [https://doi.org/10.1016/0043-1354\(95\)00107-V](https://doi.org/10.1016/0043-1354(95)00107-V)
30. Fotidis IA, Karakashev D, Kotsopoulos TA, Martzopoulos GG, Angelidaki I. Effect of ammonium and acetate on methanogenic pathway and methanogenic community composition. *FEMS Microbiology Ecology*. 2013; 83: 38–48. <https://doi.org/10.1111/j.1574-6941.2012.01456.x> PMID: 22809020
31. Habtewold J, Gordon R, Sokolov V, VanderZaag A, Wagner-Riddle C, Dunfield K. Reduction in methane emissions from acidified dairy slurry is related to inhibition of methanosarcina species. *Frontiers in Microbiology*. 2018; 9: 1–12.
32. Wang H-Z, Yan Y-C, Gou M, Yi Y, Xia Z-Y, Nobu MK, et al. Response of Propionate-Degrading Methanogenic Microbial Communities to Inhibitory Conditions. *Applied Biochemistry and Biotechnology*. 2019. <https://doi.org/10.1007/s12010-019-03005-1> PMID: 30972704
33. Liamleam W, Annachatre AP. Electron donors for biological sulfate reduction. *Biotechnology Advances*. 2007; 25: 452–463. <https://doi.org/10.1016/j.biotechadv.2007.05.002> PMID: 17572039
34. Muyzer G, Stams AJM. The ecology and biotechnology of sulphate-reducing bacteria. *Nature Reviews Microbiology*. 2008; 6: 441–454. <https://doi.org/10.1038/nrmicro1892> PMID: 18461075
35. Ottosen LDM, Poulsen H V., Nielsen DA, Finster K, Nielsen LP, Revsbech NP. Observations on microbial activity in acidified pig slurry. *Biosystems Engineering*. 2009; 102: 291–297. <https://doi.org/10.1016/j.biosystemseng.2008.12.003>
36. Fedorovich V, Lens P, Kalyuzhnyi S. Extension of Anaerobic Digestion Model No. 1. *Applied Biochemistry And Biotechnology*. 2003; 109. <https://doi.org/10.1385/abab:109:1-3:33> PMID: 12794282
37. Petersen SO, Højberg O, Poulsen M, Schwab C, Eriksen J. Methanogenic community changes, and emissions of methane and other gases, during storage of acidified and untreated pig slurry. *Journal of Applied Microbiology*. 2014; 117: 160–172. <https://doi.org/10.1111/jam.12498> PMID: 24636626
38. Rittmann BE, McCarty PL. *Environmental biotechnology: principles and applications*. McGraw-Hill; 2001.
39. Liu S, Yang F, Gong Z, Meng F, Chen H, Xue Y, et al. Application of anaerobic ammonium-oxidizing consortium to achieve completely autotrophic ammonium and sulfate removal. *Bioresour Technol*. 2008; 99: 6817–6825. <https://doi.org/10.1016/j.biortech.2008.01.054> PMID: 18343660
40. Sommer SG, Petersen SO, Søgaard HT. Greenhouse gas emission from stored livestock slurry. *Journal of Environmental Quality*. 2000; 29: 744–751. <https://doi.org/10.2134/jeq2000.00472425002900030009x>
41. Nielsen DA, Schramm A, Nielsen LP, Revsbech NP. Seasonal Methane Oxidation Potential in Manure Crusts. *Appl Environ Microbiol*. 2013; 79: 407–410. <https://doi.org/10.1128/AEM.02278-12> PMID: 23104415
42. Petersen SO, Amon B, Gattinger A. Methane Oxidation in Slurry Storage Surface Crusts. *Journal of Environmental Quality*. 2005; 34: 455–461. <https://doi.org/10.2134/jeq2005.455> PMID: 15758097

43. Vavilin VA, Fernandez B, Palatsi J, Flotats X. Hydrolysis kinetics in anaerobic degradation of particulate organic material: An overview. *Waste Management*. 2008; 28: 939–951. <https://doi.org/10.1016/j.wasman.2007.03.028> PMID: 17544638
44. Zeeman G. Methane production/emission in storages for animal manure. *Fertilizer Research*. 1994; 37: 207–211. <https://doi.org/10.1007/BF00748939>
45. Giraldo-Gomez E. Kinetics of anaerobic treatment: A critical review. *Critical Reviews in Environmental Control*. 1991; 21: 411–490. <https://doi.org/10.1080/10643389109388424>
46. Hill DT. Methane productivity of the major animal waste types. *Transactions of the American Society of Agricultural Engineers*. 1984; 27: 530–534. <https://doi.org/10.13031/2013.32822>
47. Dalby F, Fuchs A, Feilberg A. Methanogenic pathways and  $\delta^{13}\text{C}$  values from swine manure with a cavity ring-down spectrometer: Ammonia cross-interference and carbon isotope labeling. *Rapid Communications in Mass Spectrometry*. 2020; 34: 1–13. <https://doi.org/10.1002/rcm.8628> PMID: 31658498
48. Habtewold J, Gordon R, Sokolov V, VanderZaag A, Wagner-Riddle C, Dunfield K. Targeting bacteria and methanogens to understand the role of residual slurry as an inoculant in stored liquid dairy manure. *Applied and Environmental Microbiology*. 2018; 84: 1–15. <https://doi.org/10.1128/AEM.02830-17> PMID: 29374043
49. Conrad R. Importance of hydrogenotrophic, acetoclastic and methylotrophic methanogenesis for methane production in terrestrial, aquatic and other anoxic environments: A mini review. *Pedosphere*. 2020; 30: 25–39. [https://doi.org/10.1016/S1002-0160\(18\)60052-9](https://doi.org/10.1016/S1002-0160(18)60052-9)
50. Hattori S. Syntrophic acetate-oxidizing microbes in methanogenic environments. *Microbes and Environments*. 2008; 23: 118–127. <https://doi.org/10.1264/jisme.23.118> PMID: 21558697
51. Angelidaki I, Ellegaard L, Ahring BK. A comprehensive model of anaerobic bioconversion of complex substrates to biogas. *Biotechnology and Bioengineering*. 1999; 63: 363–372. PMID: 10099616
52. Dalby FR, Hafner SD, Petersen SO, VanderZaag AC, Habtewold J, Dunfield K, et al. Understanding methane emission from stored animal manure: A review to guide model development. *Journal of Environmental Quality*. 2021. <https://doi.org/10.1002/jeq2.20252> PMID: 34021608
53. Massé DI, Cata Saady NM. Psychrophilic dry anaerobic digestion of dairy cow feces: Long-term operation. *Waste Management*. 2015; 36: 86–92. <https://doi.org/10.1016/j.wasman.2014.10.032> PMID: 25434732
54. Kip N, Jansen S, Leite MFA, De Hollander M, Afanasyev M, Kuramae EE, et al. Methanogens predominate in natural corrosion protective layers on metal sheet piles. *Scientific Reports*. 2017; 7: 1–11.
55. Jensen MB, Strübing D, de Jonge N, Nielsen JL, Ottosen LDM, Koch K, et al. Stick or leave—Pushing methanogens to biofilm formation for ex situ biomethanation. *Bioresource Technology*. 2019; 291: 121784. <https://doi.org/10.1016/j.biortech.2019.121784> PMID: 31344638
56. Gomez-Alvarez V, Revetta RP, Domingo JWS. Metagenome analyses of corroded concrete wastewater pipe biofilms reveal a complex microbial system. *BMC Microbiology*. 2012;12.
57. Rosso L, Lobry JR, Flandrois JP. An Unexpected Correlation between Cardinal Temperatures of Microbial Growth Highlighted by a New Model. *Journal of Theoretical Biology*. 1993; 162: 447–463. <https://doi.org/10.1006/jtbi.1993.1099> PMID: 8412234
58. Donoso-Bravo A, Retamal C, Carballa M, Ruiz-Filippi G, Chamy R. Influence of temperature on the hydrolysis, acidogenesis and methanogenesis in mesophilic anaerobic digestion: Parameter identification and modeling application. *Water Science and Technology*. 2009; 60: 9–17. <https://doi.org/10.2166/wst.2009.316> PMID: 19587397
59. Hinshelwood CN. The Chemical Kinetics of the Bacterial Cell. *Cancer Research*. 1947; 7: 548 LP– 548.
60. Lin CY, Noike T, Sato K, Matsumoto J. Temperature Characteristics of the Methanogenesis Process in Anaerobic Digestion. *Water Science and Technology*. 1987; 19: 299–300. <https://doi.org/10.2166/wst.1987.0210>
61. Henze M, Grady CPL, Gujer W, Matsuo T. Activated Sludge Model No. 1. IAWPRC; 1987.
62. Petersen EE. Chemical Reaction Analysis. Prentice-Hall; 1965.
63. Astals S, Peces M, Batstone DJ, Jensen PD, Tait S. Characterising and modelling free ammonia and ammonium inhibition in anaerobic systems. *Water Research*. 2018; 143: 127–135. <https://doi.org/10.1016/j.watres.2018.06.021> PMID: 29940358
64. Dalby FR, Hansen MJ, Feilberg A, Kümmel S, Nikolausz M. Effect of tannic acid combined with fluoride and lignosulfonic acid on anaerobic digestion in the agricultural waste management chain. *Bioresource Technology*. 2020; 307: 123171. <https://doi.org/10.1016/j.biortech.2020.123171> PMID: 32203867
65. Jabłoński S, Rodowicz P, Łukaszewicz M. Methanogenic archaea database containing physiological and biochemical characteristics. *International Journal of Systematic and Evolutionary Microbiology*. 2015; 65: 1360–1368. <https://doi.org/10.1099/ijs.0.000065> PMID: 25604335

66. Im S, Petersen SO, Lee D, Kim DH. Effects of storage temperature on CH<sub>4</sub> emissions from cattle manure and subsequent biogas production potential. *Waste Management*. 2020; 101: 35–43. <https://doi.org/10.1016/j.wasman.2019.09.036> PMID: 31586875
67. Jarvis GN, Strömpl C, Burgess DM, Skillman LC, Moore ERB, Joblin KN. Isolation and identification of ruminal methanogens from grazing cattle. *Current Microbiology*. 2000; 40: 327–332. <https://doi.org/10.1007/s002849910065> PMID: 10706664
68. Barret M, Gagnon N, Topp E, Masse L, Massé DI, Talbot G. Physico-chemical characteristics and methanogen communities in swine and dairy manure storage tanks: Spatio-temporal variations and impact on methanogenic activity. *Water Research*. 2013; 47: 737–746. <https://doi.org/10.1016/j.watres.2012.10.047> PMID: 23206501
69. Massé D I., Masse L, Claveau S, Benchaar C, Thomas O. Methane Emissions from Manure Storages. *Transactions of the ASABE*. 2008; 51: 1775–1781. <https://doi.org/10.13031/2013.25311>
70. Weinrich S. Praxisnahe Modellierung von Biogasanlagen: systematische Vereinfachung des Anaerobic Digestion Model No. 1 (ADM1) (Practical modeling of biogas plants: systematic simplification of the Anaerobic Digestion Model No. 1 (ADM1)). PhD, Universität Rostock. 2018. [https://doi.org/10.18453/rosdok\\_id00002016](https://doi.org/10.18453/rosdok_id00002016)
71. Weinrich S, Nelles M. Systematic simplification of the Anaerobic Digestion Model No. 1 (ADM1)—Model development and stoichiometric analysis. *Bioresource Technology*. 2021; 333: 125124. <https://doi.org/10.1016/j.biortech.2021.125124> PMID: 33910118
72. Ozbayram EG, Kleinstaub S, Nikolausz M. Biotechnological utilization of animal gut microbiota for valorization of lignocellulosic biomass. *Applied Microbiology and Biotechnology*. 2020; 104: 489–508. <https://doi.org/10.1007/s00253-019-10239-w> PMID: 31797006
73. Söllinger A, Tveit AT, Poulsen M, Noel SJ, Bengtsson M, Bernhardt J, et al. Holistic Assessment of Rumen Microbiome Dynamics through Quantitative Metatranscriptomics Reveals Multifunctional Redundancy during Key Steps of Anaerobic Feed Degradation. *mSystems*. 2018; 3: 1–19. <https://doi.org/10.1128/mSystems.00038-18> PMID: 30116788
74. Demirel B, Scherer P. The roles of acetotrophic and hydrogenotrophic methanogens during anaerobic conversion of biomass to methane: A review. *Reviews in Environmental Science and Biotechnology*. 2008; 7: 173–190. <https://doi.org/10.1007/s11157-008-9131-1>
75. Hao LP, Lü F, He PJ, Li L, Shao LM. Predominant contribution of syntrophic acetate oxidation to thermophilic methane formation at high acetate concentrations. *Environmental Science and Technology*. 2011; 45: 508–513. <https://doi.org/10.1021/es102228v> PMID: 21162559
76. Batstone DJ, Karakashev D, Batstone DJ, Trably E, Angelidaki I. Acetate Oxidation Is the Dominant Methanogenic Pathway from Acetate in the Absence of Methanosaeataceae. 2014; 72: 5138–5141. <https://doi.org/10.1128/AEM.00489-06> PMID: 16820524
77. Yenigün O, Demirel B. Ammonia inhibition in anaerobic digestion: A review. *Process Biochemistry*. 2013; 48: 901–911. <https://doi.org/10.1016/j.procbio.2013.04.012>
78. Hafner SD, Koch K, Carrere H, Astals S, Weinrich S, Rennuit C. Software for biogas research: Tools for measurement and prediction of methane production. *SoftwareX*. 2018; 7: 205–210. <https://doi.org/10.1016/j.softx.2018.06.005>
79. Markfoged R. Microbial Control of Gas-Exchange at Air-Manure Interfaces. Aarhus University. 2013.
80. R Core Team. R: A Language and Environment for Statistical Computing. Vienna, Austria: R Foundation for Statistical Computing; 2021. <https://www.R-project.org/>
81. Raposo F, Borja R, Ibelli-Bianco C. Predictive regression models for biochemical methane potential tests of biomass samples: Pitfalls and challenges of laboratory measurements. *Renewable and Sustainable Energy Reviews*. 2020; 127. <https://doi.org/10.1016/j.rser.2020.109890>
82. Møller HB, Sommer SG, Ahring BK. Methane productivity of manure, straw and solid fractions of manure. *Biomass and Bioenergy*. 2004; 26: 485–495. <https://doi.org/10.1016/j.biombioe.2003.08.008>
83. Møller HB, Sommer SG, Ahring BK. Biological Degradation and Greenhouse Gas Emissions during Pre-Storage of Liquid Animal Manure. *Journal of Environmental Quality*. 2004; 33: 27–36. <https://doi.org/10.2134/jeq2004.2700> PMID: 14964355
84. Petersen SO, Olsen AB, Elsgaard L, Triolo JM, Sommer SG. Estimation of methane emissions from slurry pits below pig and cattle confinements. *PLoS ONE*. 2016; 11: 1–16. <https://doi.org/10.1371/journal.pone.0160968> PMID: 27529692
85. Choorit W, Wisarnwan P. Effect of temperature on the anaerobic digestion of palm oil mill effluent. *Electronic Journal of Biotechnology*. 2007; 10: 376–385.
86. Rolfe MD, Rice CJ, Lucchini S, Pin C, Thompson A, Cameron ADS, et al. Lag phase is a distinct growth phase that prepares bacteria for exponential growth and involves transient metal accumulation. *Journal of Bacteriology*. 2012; 194: 686–701. <https://doi.org/10.1128/JB.06112-11> PMID: 22139505

87. Hashimoto A. Methane from swine manure: Effect of temperature and influent substrate concentration on kinetic parameter (K). *Agricultural Wastes*. 1984; 9: 299–308. [https://doi.org/10.1016/0141-4607\(84\)90088-X](https://doi.org/10.1016/0141-4607(84)90088-X)
88. Oude Elferink JW, Visser A, Pol LWH, Stams AJM. Sulfate reduction in methanogenic bioreactors. *FEMS Microbiology Reviews*. 1994; 15: 119–136. <https://doi.org/10.1111/j.1574-6976.1994.tb00130.x>
89. VanderZaag AC, Baldé H, Habtewold J, Le Riche EL, Burt S, Dunfield K, et al. Intermittent agitation of liquid manure: effects on methane, microbial activity, and temperature in a farm-scale study. *Journal of the Air and Waste Management Association*. 2019; 69: 1096–1106. <https://doi.org/10.1080/10962247.2019.1629359> PMID: 31184562